07.2;07.3

Impact of transverse optical confinement on performance of 1.55 μm vertical-cavity surface-emitting lasers with a buried tunnel junction

© S.A. Blokhin[1], M.A. Bobrov[1], A.A. Blokhin[1], N.A. Maleev[1], A.G. Kuzmenkov[2], A.P. Vasyl'ev[2], S.S. Rochas[3], A.V. Babichev[3], I.I. Novikov[3], L.Ya. Karachinsky[3], A.G. Gladyshev[4], D.V. Denisov[5], K.O. Voropaev[6], A.Yu. Egorov[4], V.M. Ustinov[2]

[1] Ioffe Institute, St. Petersburg, Russia
[2] Submicron Heterostructures for Microelectronics, Research and Engineering Center, Russian Academy of Sciences, St. Petersburg, Russia
[3] ITMO University, St. Petersburg, Russia
[4] Connector Optics LLC, St. Petersburg, Russia
[5] St. Petersburg State Electrotechnical University „LETI", St. Petersburg, Russia
[6] OAO OKB-Planeta, Veliky Novgorod, Russia
E-mail: blokh@mail.ioffe.ru

Received June 30, 2021
Revised July 19, 2021
Accepted July 20, 2021

The impact of transverse optical confinement on the static and spectral characteristics of 1.55 μm vertical-cavity surface-emitting lasers (WF-VCSEL) with a buried tunnel junction (BTJ) n^{++}-InGaAs/p^{++}-InGaAs/p^{++}-InAlGaAs, implemented using molecular-beam epitaxy and wafer fusion. It was found that for VCSELs with a tunnel junction (TJ) etching depth of 15 nm, the single-mode lasing occurs up to 8 μm BTJ mesa size due to a relatively weak lateral optical confinement, while the effect of a saturable absorber (SA) appears when the BTJ mesa size is less than 7 μm. Enhancing lateral optical confinement by increasing the BTJ etching depth up to 20 nm leads to suppression of the SA effect at the BTJ mesa size of 5−6 μm, but simultaneously limits the maximum single-mode optical power. According to obtained results an increase in the spectral mismatch between the maximum of the gain spectrum of the active region and the resonance wavelength of the WF-VCSEL up to $\sim$ 35−50 nm will make it possible to suppress the undesirable SA effect in a wide range of the BTJ mesa sizes maintaining the single-mode lasing.

Keywords: vertical-cavity surface-emitting laser, wafer fusion, molecular beam epitaxy, single-mode operation, saturable absorber.

DOI: 10.21883/TPL.2022.14.55117.18942

The problem of fabrication of efficient single-mode vertical-cavity surface-emitting lasers (VCSELs) operating in the 1.55 μm range still remains topical. The most promising approach here consists in combining a high-efficiency InAlGaAsP/InP active region with distributed Bragg reflectors (DBRs) based on materials with a high contrast of refraction indices and a fine thermal conductivity. This approach is implemented in the wafer fusion (hereinafter referred to as WF-VCSELs) technology [1–3], which combines the advantages of InAlGaAsP/InP and AlGaAs/GaAs material systems, and in the technology of hybrid integration with high-contrast dielectric DBRs (hybrid VCSELs) [4–6].

Such lasers feature vertical microcavities with intracavity contact (IC) layers and a buried tunnel junction (BTJ) based on n^{++}/p^{++}-In(Al)GaAs layers. Tunnel junctions (TJs) with optically transparent InAlGaAs layers [1,2] or TJs based on n^{++}-InGaAs/p^{++}-InAlGaAs layers [4,5], where intrinsic absorption in n^{++}-InGaAs layers may be neglected by virtue of the Burstein−Moss effect, are used most often to suppress optical absorption in long-wave VCSELs. An efficient *in situ* removal of oxides from the surface of Al-containing layers at standard temperatures is hard to implement in molecular beam epitaxy (MBE). In view of this, chemical beam epitaxy (CBE) [4,7] or, most commonly, metalorganic chemical vapor deposition (MOCVD) [1,5] are used for regrowth of the TJ surface relief. It should be noted that the difficulty of reaching high levels of p doping of p^{++}-InGaAs layers with the use of dopant impurities resistant to segregation (e.g., carbon) [8] is another reason why n^{++}/p^{++}-InAlGaAs TJs are chosen for MOCVD. Within the BTJ concept, transverse optical confinement, which defines the modal composition of VCSEL emission is effected by a height difference between the BTJ region and the peripheral region of a backward-biased $p^{+}-n$ junction. Specifically, if a n^{++}-InGaAs/p^{++}-InAlGaAs TJ (with a typical etching depth of 20 nm) is used and a BTJ is formed by CBE, the effective refraction index contrast in the hybrid VCSEL structure reaches a level of 0.03 [8], and the resulting strong waveguide effect limits the BTJ mesa size at which stable fundamental-mode lasing is achieved to 4−5 μm [4]. If MOCVD is used for regrowth of the TJ surface relief, single-mode lasing in hybrid VCSELs persists up to a BTJ mesa size of $\sim$ 6 μm [5] due to partial planarization. This is indicative of weakening of

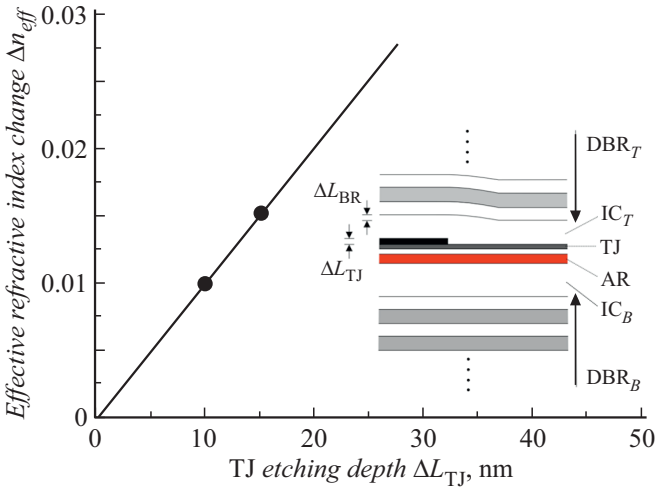

Figure 1. Results of modeling of effective refraction index contrast Δn_{eff} as a function of etching depth ΔL_{TJ} of a composite TJ for a 1.55 μm WF-VCSEL. Circles denote the data for lasers tested in experiments. The schematic diagram of a transverse section of the WF-VCSEL heterostructure in the microcavity region is shown in the inset. DBR_T and DBR_B are top and bottom DBRs, IC_T and IC_B are top and bottom IC layers, AR is the active region, and TJ is the tunnel junction.

the waveguide effect. It has been demonstrated that the use of MOCVD for regrowth of the n^{++}/p^{++}-InAlGaAs TJ surface relief (with a typical etching depth of ~ 25 nm) provides an opportunity to raise output optical power P_{SM} of VCSELs in single-mode operation to a level of 6.0−6.5 mW at a BTJ mesa size of 6−7 μm [1]. A further expansion of the BTJ mesa size range and the potential to increase output power P_{SM} are associated with the introduction of an additional loss mechanism for higher-order modes due to the formation of spatial relief in the top *n*-InP IC layer at the fused interface in VCSELs [9] or with the suppression of spatial hole burning due to the formation of surface relief in the InGaAs contact layer of hybrid VCSELs with a short cavity [6].

We have recently proposed a TJ structure based on n^{++}-InGaAs/p^{++}-InGaAs/p^{++}-InAlGaAs layers (hereinafter referred to as a composite TJ) that provides an opportunity to use MBE at all stages of fabrication of the WF-VCSEL heterostructure and construct lasers operating at 1.3 and 1.55 μm with parameters comparable to those of WF-VCSELs based on n^{++}/p^{++}-InAlGaAs TJs [10,11]. The MBE method is distinct in that it preserves height difference ΔL_{BR} in the regrown surface morphology (see the inset of Fig. 1). Therefore, it is of great interest to examine the waveguide effect in these WF-VCSELs.

In the present study, we investigate and analyze the influence of the transverse optical confinement on the modal composition and device characteristics of 1.55 μm WF-VCSELs based on n^{+}-InGaAs/p^{+}-InGaAs/p^{+}-InAlGaAs BTJs fabricated using MBE and wafer fusion.

The studied VCSELs comprise a GaAs substrate a bottom DBR based on 35.5 pairs of GaAs/AlGaAs layers, a bottom *n*-InP IC layer with a contact *n*-InGaAsP layer, an active region based on strained InGaAs/InAlGaAs quantum wells, a *p*-InAlAs emitter, a n^{++}-InGaAs/p^{++}-InGaAs/p^{++}-InAlGaAs BTJ, a top *n*-InP IC layer with a contact *n*-InGaAsP layer, and a top DBR based on 20.5 pairs of GaAs/AlGaAs layers. TJ layers, contact layers, and fused interfaces are positioned at the minima of the longitudinal intensity distribution of the electromagnetic field for the fundamental mode in order to weaken the waveguide effect, which is induced by the BTJ mesa formation, minimize free-carrier absorption in doped layers and interband absorption, and suppress light scattering off InGaAsP−GaAs fused interfaces. The design value of spectral mismatch between the resonance wavelength of the WF-VCSEL microcavity and the gain peak of the active region (the so-called gain-to-cavity detuning) is around 20 nm. In the case of a composite TJ, the n^{++}-InGaAs layer thickness sets the minimum etching depth, while the net thickness of n^{++}-InGaAs and p^{++}-InGaAs layers specifies the maximum etching depth. Therefore, the studied VCSEL designs differed only in the n^{++}-InGaAs layer thickness, while the thicknesses of p^{++}-InGaAs and p^{++}-InAlGaAs layers remained fixed. The design of lasers and the specifics of their fabrication were discussed in detail in [10,12,13].

In contrast to MOCVD, MBE regrowth does not induce even partial planarization of the surface relief ($\Delta L_{BR} = \Delta L_{TJ}$). This makes it easy to estimate the optical confinement level using the model of an effective refraction index [14] and the design value of the relief height difference. Figure 1 presents the calculated value of effective refraction index contrast Δn_{eff} as a function of etching depth ΔL_{TJ} of a composite TJ for the studied WF-VCSELs within the model of an effective cylindrical waveguide with a one-step refraction index change [15]. The results of calculation of the normalized frequency (V number) demonstrate that the considered effective waveguide with contrast $\Delta n_{eff} \sim 0.0035$ is single-mode at BTJ mesa sizes up to 8 μm. At higher contrast values, the limit BTJ mesa size for single-mode operation decreases: 6 μm at $\Delta n_{eff} \sim 0.0062$ and less than 4 μm at $\Delta n_{eff} \sim 0.0138$. Thus, although TJ layers are positioned at the minimum of the electromagnetic field of the fundamental mode, the waveguide effect even at relatively shallow TJ etching depths is stronger than in classical near-IR (In)AlGaAs/GaAs VCSELs with an oxide current aperture [16]. At the same time, the effective refraction index contrast in lithographic near-IR (In)AlGaAs/GaAs VCSELs, where the procedure of etching and regrowth of an intracavity phase-shifting layer is performed for current and optical confinement, is considerably higher than the value of Δn_{eff} for WF-VCSELs at comparable etching depths [17].

According to the experimental data from Fig. 2, *a*, WF-VCSELs with a design value of $\Delta n_{eff} \sim 0.01$ demonstrate single-mode lasing up to a BTJ size of 8 μm with a side-mode suppression ratio (SMSR) in excess of 50 dB. Optical

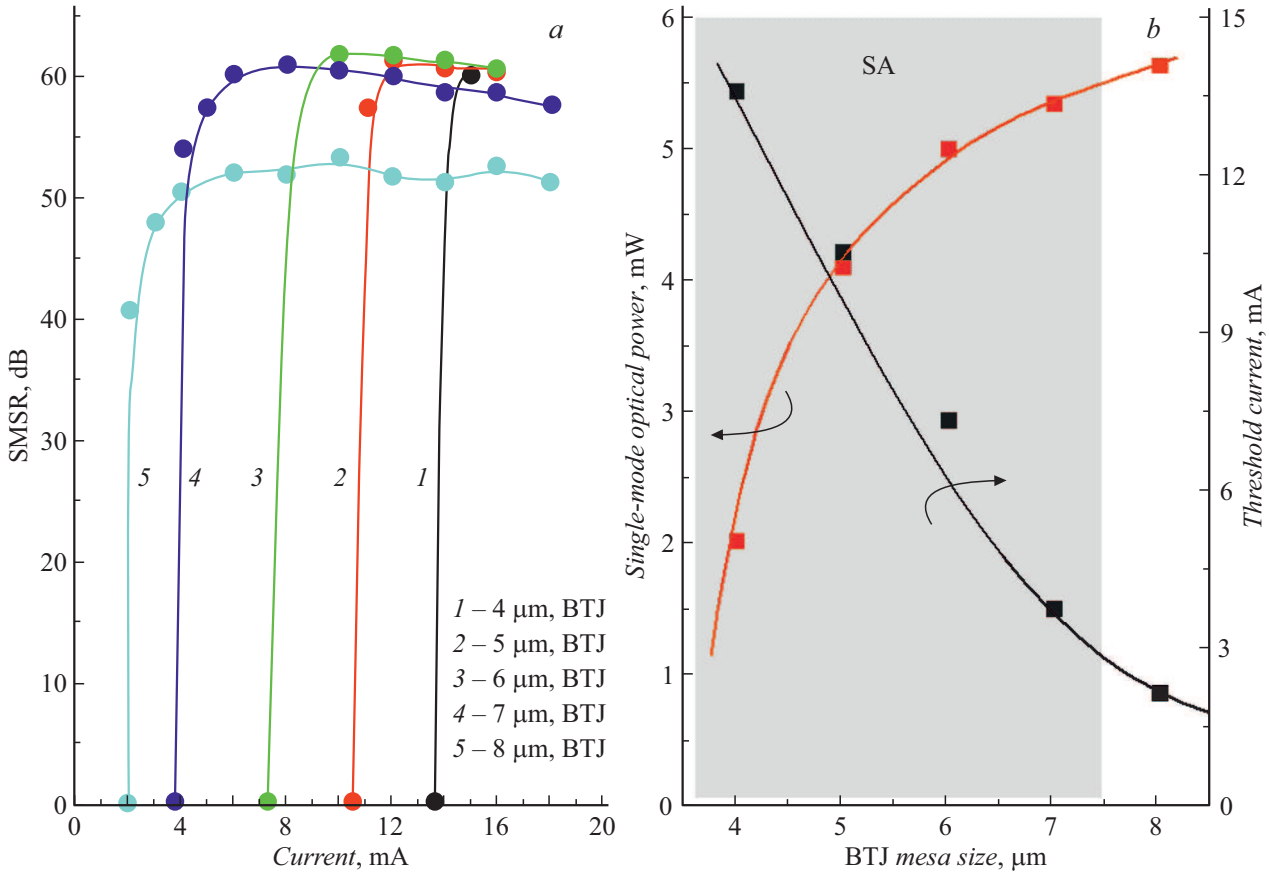

Figure 2. WF-VCSELs of the 1.55 μm range with a design value of $\Delta n_{eff} \sim 0.01$. *a* — Dependences of SMSR on current for different BTJ mesa sizes; *b* — dependences of threshold current I_{th} and the maximum optical power in single-mode operation P_{SM} on the BTJ mesa size. Measurements were performed at a temperature of 20°C. The gray area is the region where the SA effect is observed.

power P_{SM} increases with BTJ mesa size and reaches 5.6 mW for a mesa 8 μm in size (Fig. 2, *b*). At the same time, threshold current I_{th} increases rapidly as the BTJ mesa becomes smaller (Fig. 2, *b*), thus inducing significant narrowing of the operating current range for small-sized BTJ mesas (Fig. 2, *a*) and affecting negatively the dynamic characteristics of lasers (not shown). This behavior is apparently attributable to an increase in lateral dimensions of regrown relief (see the inset in Fig. 1), which results in the formation of an effective waveguide with a gradient refraction index profile. This leads, on the one hand, to a sharp reduction in the transverse optical confinement factor for higher-order modes in the case of large-sized BTJ mesas and, on the other hand, to a reduction in the transverse optical confinement factor for the fundamental mode and the emergence of a saturated absorber (SA) effect, which is characterized by a stepwise variation of optical power with current and a small hysteresis region [18], in unpumped parts of the active region.

In the case of WF-VCSELs with a design value of $\Delta n_{eff} \sim 0.015$, an enhancement of optical contrast Δn_{eff} of the effective waveguide translates into a reduction in the maximum SMSR value with increasing BTJ mesa size and into narrowing of the BTJ mesa size range in which single-mode lasing is sustained throughout the entire range of currents. These behavior are also typical of VCSELs with an oxide current aperture [16] and lithographic [17] and hybrid [6] VCSELs. In the present study, the limit SMSR value exceeds 50 dB for lasers with a BTJ mesa smaller than 6 μm and decreases to a level of 38 dB in lasers with a BTJ mesa size of 8 μm; in the latter case, the SMSR value drops sharply at currents in excess of 5 mA, and single-mode lasing gives way to multi-mode operation (Fig. 3, *a*). Thus, optical power P_{SM} reaches its maximum of ~ 5.2 mW at a BTJ mesa size of 7 μm (Fig. 3, *b*). In addition, the enhancement of optical confinement translates into suppression of the SA effect at intermediate BTJ mesa sizes and makes the growth of threshold current I_{th} for small-sized BTJ mesas less steep (Fig. 3, *b*). This provides evidence in favor of the proposed cause and mechanism of SA formation.

It should be noted that a further increase in the etching depth for a composite TJ appears to be impractical. Although deeper etching should facilitate further suppression of the SA effect and reduction of threshold currents for BTJ mesas smaller than 6 μm, thus having a beneficial effect on the dynamic parameters of lasers, it is also associated with a further reduction of the limit BTJ mesa size for single-

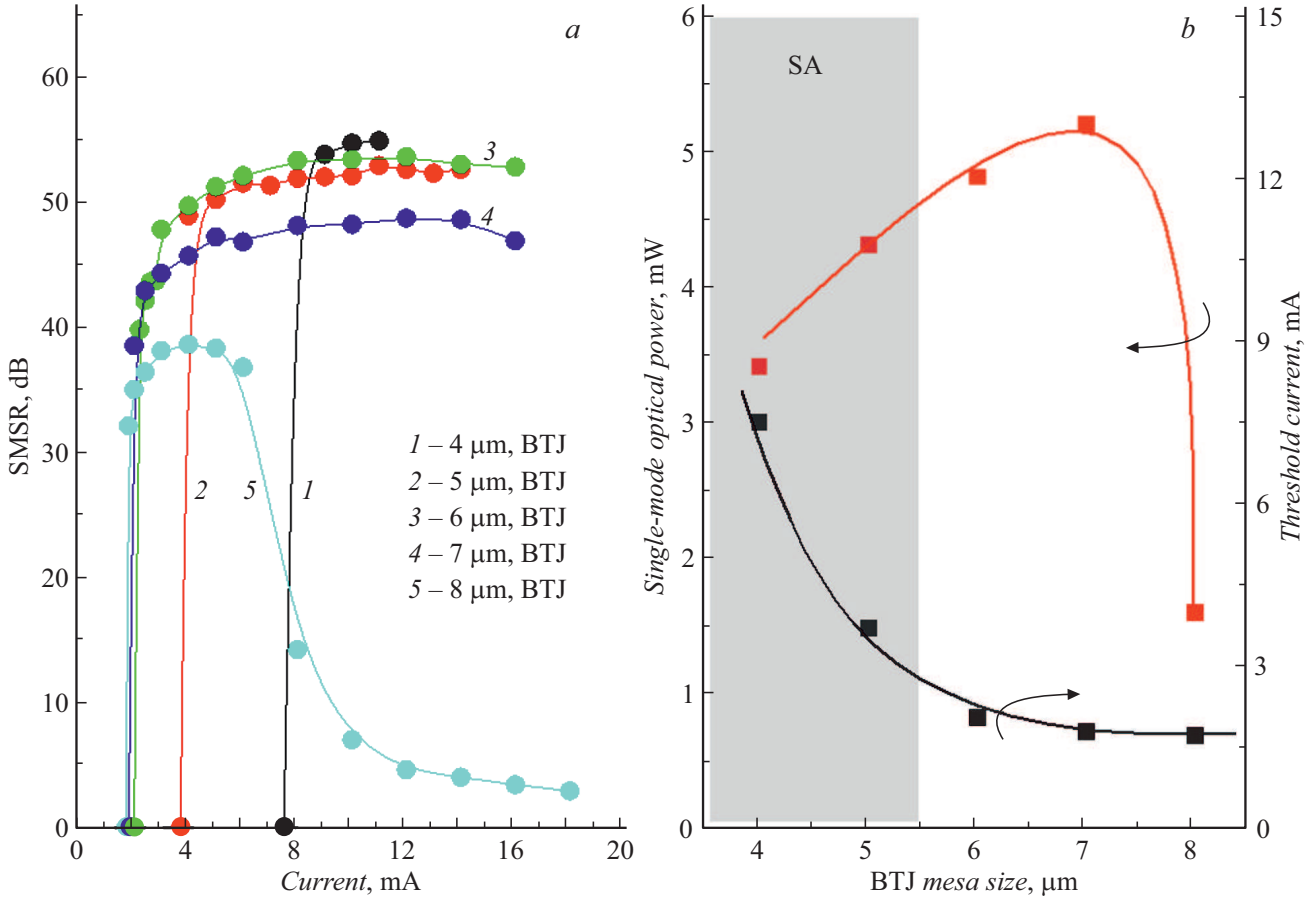

Figure 3. WF-VCSELs of the 1.55 μm range with a design value of $\Delta n_{eff} \sim 0.015$. *a* — Dependences of SMSR on current for different BTJ mesa sizes; *b* — dependences of threshold current I_{th} and the maximum optical power in single-mode operation P_{SM} on the BTJ mesa size. Measurements were performed at a temperature of 20°C. The gray area is the region where the SA effect is observed.

mode lasing. Coupled with an enhancement of thermal resistance, this should impose event stricter constraints on maximum optical power P_{SM}. In view of the enhancement of the SA effect at higher temperatures, it is fair to assume that a two-fold increase in the design gain-to-cavity detuning should provide an opportunity to reduce absorption at the resonance VCSEL wavelength in unpumped parts of the active region, suppress the SA effect additionally, and improve the thermal stability of WF-VCSELs.

Thus, the influence of transverse optical confinement on the static and spectral characteristics of 1.55 μm WF-VCSELs fabricated using molecular beam epitaxy and wafer fusion was examined. The optical confinement level was set by the etching depth of a composite n^{++}-InGaAs/p^{++}-InGaAs/p^{++}-InAlGaAs TJ and calculated as effective refraction index contrast Δn_{eff}. Stable single-model lasing was achieved in lasers with a low optical confinement level ($\Delta n_{eff} \sim 0.01$) in a wide range of BTJ mesa sizes (4–8 μm) due to an increase in lateral dimensions of regrown surface relief, but the absorption of light in unpumped parts of the active region induced an unwanted SA effect for BTJ mesas smaller than 7 μm. Raising contrast Δn_{eff} to ~ 0.015, one may suppress the SA effect at intermediate BTJ mesa sizes (5–6 μm), but this imposes constraints on the limit BTJ mesa size for fundamental-mode lasing and on the maximum output optical power in single-mode operation. An enhancement of gain-to-cavity detuning should provide an opportunity to improve the thermal stability of lasers and suppress the SA effect further while maintaining the efficient single-mode operation regime.

Conflict of interest

The authors declare that they have no conflict of interest.

References

[1] A. Caliman, A. Mereuta, G. Suruceanu, V. Iakovlev, A. Sirbu, E. Kapon, Opt. Express, **19** (18), 16996 (2011). DOI: 10.1364/OE.19.016996

[2] D. Ellafi, V. Iakovlev, A. Sirbu, G. Suruceanu, Z. Mickovic, A. Caliman, A. Mereuta, E. Kapon, IEEE J. Sel. Top. Quant. Electron., **21** (6), 414 (2015). DOI: 10.1109/jstqe.2015.2412495

[3] A.V. Babichev, L.Ya. Karachinsky, I.I. Novikov, A.G. Gladyshev, S.A. Blokhin, S. Mikhailov, V. Iakovlev, A. Sirbu, G. Stepniak, L. Chorchos, J.P. Turkiewicz, K.O. Voropaev, A.S. Ionov, M. Agustin, N.N. Ledentsov, A.Yu. Egorov, IEEE J. Sel. Top. Quant. Electron., **53** (6), 2400808 (2017). DOI: 10.1109/JQE.2017.2752700
[4] C. Lauer, M. Ortsiefer, R. Shau, J. Rosskopf, G. Bohm, R. Meyer, M.C. Amann, Phys. Status Solidi C, **1** (8), 2183 (2004). DOI: 10.1002/pssc.200404770
[5] M. Müller, W. Hofmann, T. Grundl, M. Horn, P. Wolf, R.D. Nagel, E. Ronneberg, G. Böhm, D. Bimberg, M.-C. Amann, IEEE J. Sel. Top. Quant. Electron., **17** (5), 1158 (2011). DOI: 10.1109/JSTQE.2011.2109700
[6] T. Gründl, P. Debernardi, M. Müller, C. Grasse, P. Ebert, K. Geiger, M. Ortsiefer, G. Bohm, R. Meyer, M.-C. Amann, IEEE J. Sel. Top. Quant. Electron., **19** (4), 1700913 (2013). DOI: 10.1109/JSTQE.2013.2244572
[7] M. Ortsiefer, R. Shau, G. Bohm, F. Kohler, M.C. Amann, Appl. Phys. Lett., **76** (16), 2179 (2000). DOI: 10.1049/el:20020819
[8] D. Keiper, R. Westphalen, G. Landgren, J. Cryst. Growth, **197** (1-2), 25 (1999). DOI: 10.1016/S0022-0248(98)00903-8
[9] N. Volet, T. Czyszanowski, J. Walczak, L. Mutter, B. Dwir, Z. Micković, P. Gallo, A. Caliman, A. Sirbu, A. Mereuta, V. Iakovlev, E. Kapon, Opt. Express, **21** (22), 26983 (2013). DOI: 10.1364/OE.21.026983
[10] S.A. Blokhin, M.A. Bobrov, N.A. Maleev, A.A. Blokhin, A.G. Kuz'menkov, A.P. Vasil'ev, S.S. Rochas, A.G. Gladyshev, A.V. Babichev, I.I. Novikov, L.Ya. Karachinsky, D.V. Denisov, K.O. Voropaev, A.S. Ionov, A.Yu. Egorov, V.M. Ustinov, Tech. Phys. Lett., **46** (9), 854 (2020). DOI: 10.1134/S1063785020090023.
[11] S.A. Blokhin, A.V. Babichev, A.G. Gladyshev, L.Ya. Karachinsky, I.I. Novikov, A.A. Blokhin, S.S. Rochas, D.V. Denisov, K.O. Voropaev, A.S. Ionov, A.Yu. Egorov, Electron. Lett. (First published: 3 June 2021). DOI: 10.1049/ell2.12232
[12] S.A. Blokhin, V.N. Nevedomsky, M.A. Bobrov, N.A. Maleev, A.A. Blokhin, A.G. Kuzmenkov, A.P. Vasyl'ev, S.S. Rohas, A.V. Babichev, A.G. Gladyshev, I.I. Novikov, L.Ya. Karachinsky, D.V. Denisov, K.O. Voropaev, A.S. Ionov, A.Yu. Egorov, V.M. Ustinov, Semiconductors, **54** (10), 1276 (2020). DOI: 10.21883/FTP.2020.10.49947.9463 [S.A. Blokhin, S.N. Nevedomsky, M.A. Bobrov, N.A. Maleev, A.A. Blokhin, A.G. Kuzmenkov, A.P. Vasyl'ev, S.S. Rohas, A.V. Babichev, A.G. Gladyshev, I.I. Novikov, L.Ya. Karachinsky, D.V. Denisov, K.O. Voropaev, A.S. Ionov, A.Yu. Egorov, V.M. Ustinov, Semiconductors, **54** (10), 1276 (2020). DOI: 10.1134/S1063782620100048].
[13] K.O. Voropaev, B.I. Seleznev, A.Yu. Prokhorov, A.S. Ionov, S.A. Blokhin, J. Phys.: Conf. Ser., **1658**, 12069 (2020). DOI: 10.1088/1742-6596/1658/1/012069
[14] G.R. Hadley, Opt. Lett., **20** (13), 1483 (1995). DOI: 10.1364/OL.20.001483
[15] G.P. Agrawal, *Fiber-optic communication systems* (Wiley, N.Y., 2010).
[16] R. Michalzik, *VCSELs: fundamentals, technology and applications of vertical-cavity surface-emitting lasers* (Springer-Verlag, Berlin, 2013). DOI: 10.1007/978-3-642-24986-0
[17] D.G. Deppe, J. Leshin, J. Leshin, L. Eifert, F. Tucker, T. Hillyer, Electron. Lett., **53** (24), 1598 (2017). DOI: 10.1049/el.2017.2780
[18] S.A. Blokhin, M.A. Bobrov, A.A. Blokhin, A.P. Vasil'ev, A.G. Kuz'menkov, N.A. Maleev, S.S. Rochas, A.G. Gladyshev, A.V. Babichev, I.I. Novikov, L.Ya. Karachinsky, D.V. Denisov, K.O. Voropaev, A.S. Ionov, A.Yu. Egorov, V.M. Ustinov, Tech. Phys. Lett., **46** (12), 1257 (2020). DOI: 10.1134/S1063785020120172.